A MICROMECHANICAL MODELLING OF CYCLIC CREEP IN BRITTLE MATRIX COMPOSITES UNDER COMPRESSIVE LOADING

M. KOTOUL

Department of Solid Mechanics, Technical University of Brno, Technická 2, 616 69 Brno, Czech Republic

ABSTRACT

Mori-Tanaka's approach [1] is used to modelling metal particulate-reinforced brittle matrix composites under cyclic compressive loading. The J_2-flow theory is considered as the relevant physical law of plastic flow in inclusions. A strong constraint exerted by matrix on inclusions causes that even the evanescent kinematical hardening rule does not predict any ratchetting of a composite. It is shown that the weakening constraint of the matrix caused by microfracture damage around inclusions is closely coupled with the plasticity of inclusion and leads to ratchetting even when the plastic deformation of inclusions is described by an isotropic hardening rule. A detailed parametric study has revealed that ratchetting is followed by either plastic or elastic shakedown, depending on the load amplitude, composite parameters and the mean microcracks length.

KEYWORDS

Ratchetting, Low Cycle Loading, Ceramics, Microfracturing.

INTRODUCTION

Brittle solids fail in compression by a process of progressive microfracture. If subjected to cyclic loading beyond the elastic range with nonzero mean stress, usually there is a cycle by cycle accumulation of inelastic strain related to microfracturing in the direction of mean stress similarly like an accumulation of plastic strain in steels or other metals. This phenomenon is called cyclic creep or ratchetting. In cyclic plasticity of ductile materials there are several models capable to describe ratchetting, among others Armstrong-Frederick (AF) model [2], Chaboche [3], Ohno [4] and/or Jiang model [5]. AF model, however, in most situations, overpredicts ratchetting. With brittle matrix reinforced by ductile inclusions is a problem of constitutive modeling even more complicated. In ceramic matrix, for example, the nature and number of slip systems available for deformation in brittle matrix does not usually allow for macroscopic plastic strains; however, it should be recognized that microcracking in matrix per se causes significant internal displacement and can enable permanent macroscopic strains which have to be added to permanent strains exhibited by ductile inclusions. Further complication stems from the fact that brittle materials are used primarily in circumstances when the compressive stresses are prevalent and the tensile stresses are very small if not absent. Microcracking in these materials depends on the weak spots in the material and the localized stress concentrations at microstructural heterogeneities.

CONSTITUTIVE MODELLING

Summary of basic relations

Assume a representative volume element (RVE) of material. A surface traction, giving rise to an uniform stress $\overline{\sigma}_{ij}$, is prescribed to the boundary of the RVE. Following an approach proposed by Tandon and Weng [6] we consider an auxiliary problem of an identically shaped comparison material element with the property of the matrix subjected to the same traction. Consider first the case of the RVE without microcracks. The stress and strain in the comparison material, $\overline{\sigma}_{ij}$ and ε^0_{ij} respectively, are related in the rate formulation by

$$\dot{\overline{\sigma}}_{ij} = L^0_{ijkl}\,\dot{\varepsilon}^0_{kl}, \tag{1}$$

where $L^0_{ijkl} = \left(\kappa_0 - \frac{2}{3}\mu_0\right)\delta_{kl}\delta_{ij} + \mu_0\left(\delta_{ik}\delta_{jl} + \delta_{jk}\delta_{il}\right)$, where μ_0, κ_0 are shear modulus and bulk modulus of the matrix. (The following symbolic notation will be used: Greek letters denote the 2nd-rank tensors, and ordinary capital letters denote the 4-th-rank ones. The inner product of 2 tensors is written such that $\sigma : \varepsilon = \sigma_{ij}\varepsilon_{ij}$, $L : \varepsilon = L_{ijkl}\varepsilon_{kl}$, $L : A = L_{ijkl}A_{klmn}$, and $L :: A = L_{ijkl}A_{ijkl}$ in terms of the indicial components.) The stress and strain rates in Eq. (1) represent the average stress and strain rates of the matrix when it contains only a single inclusion. At finite concentration the average stress and strain rates of the matrix differ from these by $\dot{\tilde{\sigma}}$ and $\dot{\tilde{\varepsilon}}$ respectively, and are connected by

$$\dot{\overline{\sigma}} + \dot{\tilde{\sigma}} = L^0 : \left(\dot{\varepsilon}^0 + \dot{\tilde{\varepsilon}}\right). \tag{2}$$

The stress rate in the inclusion $\dot{\sigma}^{(in)}$further differs from the mean of the matrix by a perturbed value $\dot{\sigma}^{(pt)}$. The strain rate in the inclusion differs by a perturbed value $\dot{\varepsilon}^{(pt)}$. A part of $\dot{\varepsilon}^{(pt)}$is due to the actual plastic deformation rate $\dot{\varepsilon}^p$which is defined through the relevant physical laws of plastic flow. The remaining part of $\dot{\varepsilon}^{(pt)}$in the inclusion, on the other hand, is due to eigenstrains rate $\dot{\varepsilon}^*$which is introduced in order to homogenize the solid. From Eshelby's equivalence principle one has

$$\dot{\sigma}^{(in)} = \dot{\overline{\sigma}} + \dot{\tilde{\sigma}} + \dot{\sigma}^{(pt)} = L^1 : \left(\dot{\varepsilon}^0 + \dot{\tilde{\varepsilon}} + \dot{\varepsilon}^{(pt)} - \dot{\varepsilon}^p\right) = L^0 : \left(\dot{\varepsilon}^0 + \dot{\tilde{\varepsilon}} + \dot{\varepsilon}^{(pt)} - \dot{\varepsilon}^p - \dot{\varepsilon}^*\right), \tag{3}$$

where L^1 is elastic moduli tensor of the inclusion. Eshelby's solution readily renders the relation

$$\dot{\varepsilon}^{(pt)} = S : \left(\dot{\varepsilon}^p + \dot{\varepsilon}^*\right), \tag{4}$$

where S is the Eshelby tensor whose components, in the present case, depend only on the Poisson's ratio ν_0 of the matrix. Since the volume average of the mean stress in the matrix and the inclusions must be in balance with $\overline{\sigma}$, we have

$$\dot{\tilde{\sigma}} = -c\,\dot{\sigma}^{(pt)}, \tag{5}$$

where c is the volume fraction of inclusions. In view of (2) it follows from (3)

$$\dot{\sigma}^{(pt)} = L^0 : \left(\dot{\varepsilon}^{(pt)} - \dot{\varepsilon}^p - \dot{\varepsilon}^*\right). \tag{6}$$

Since $\dot{\tilde{\sigma}} = L^0 : \dot{\tilde{\varepsilon}}$ we get from (4),(5),(6)

$$\dot{\tilde{\varepsilon}} = -c\,(S - I) : \left(\dot{\varepsilon}^p + \dot{\varepsilon}^*\right), \tag{7}$$

where I is the 4th-rank identity tensor. Substituting (4) and (7) into (3) one obtains the equation

$$L^1 : \left[\dot{\varepsilon}^0 + (1-c)\, S : \left(\dot{\varepsilon}^* + \dot{\varepsilon}^p\right) + c\left(\dot{\varepsilon}^* + \dot{\varepsilon}^p\right) - \dot{\varepsilon}^p\right] = L^0 : \left(\dot{\varepsilon}^0 + (1-c)\,(S-I) : \left(\dot{\varepsilon}^* + \dot{\varepsilon}^p\right)\right), \tag{8}$$

which can be solved for $\dot{\varepsilon}^*$.

Extension of the model to microcracked composites

Let the x_1 axis coincides with the principal direction of highest applied (in the sense of the absolute value) compressive stress $\overline{\sigma}_{11}$. The x_1 axis defines the polar axis of spherical inclusions. The stresses are then concentrated by inclusions under multiaxial compressive loading such that, the hoop stresses along the interface at inclusion's north and south poles are most tensile ones. Consider now the case when microcracks are nucleated in the matrix from the matrix-inclusion interface at their north and south poles due to this local concentrated tensile field. Each inclusion gives rise to a pair of microcrack, see Fig. 1. The additional average strain rate of matrix $\dot{\overline{\varepsilon}}^{MC}$ due to microcracks is given by

$$\dot{\overline{\varepsilon}}_{ij}^{MC} = \frac{1}{V} \int\limits_{\partial\Omega^+} \frac{1}{2}\left(n_i\,[\dot{u}_j] + [\dot{u}_i]\,n_j\right) dS = H_{ijkl}\,\dot{\overline{\sigma}}_{kl}, \tag{9}$$

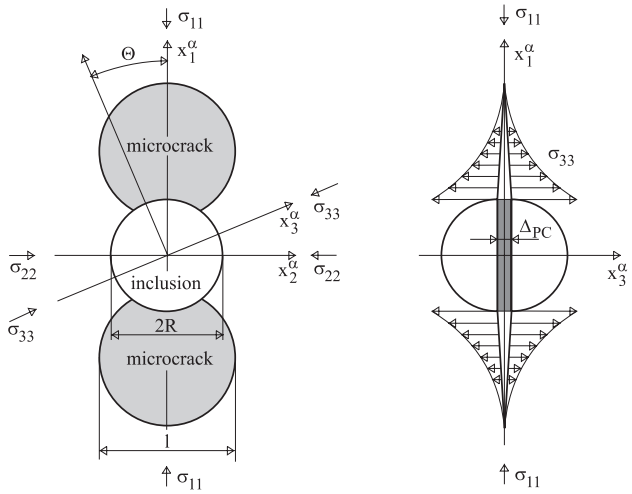

Fig. 1. Tensile stress and microcracks inception at the inclusion's poles

where the constant tensor H_{ijkl} is defined through (9), n_i is the exterior unit normal of $\partial\Omega^+$ which denotes the union of all crack "upper" surfaces, $[\dot{u}_j]$ is the microcrack-opening-displacement rate and V is the volume of RVE, see for details e.g. Nemat-Nasser and Hori [7]. (Note that microcracks are assumed not to change their size.) Apparently, all microcracks are parallel to the x_1 axis. If the lateral principal pressures $\overline{\sigma}_{22}$ and $\overline{\sigma}_{33}$ are of the same magnitude, then the distribution of the unit normals of microcracks is random in the x_2, x_3-plane and, due to the symmetry in the x_2, x_3-plane, the overall response of the RVE is transversely isotropic, with the x_1 axis being the axis of symmetry. Assume that all microcracks are approximated by penny-shaped microcracks with the same radius $\frac{l}{2}$. The distribution of the microcracks is assumed to be dilute. Let $(x_1^\alpha, x_2^\alpha, x_3^\alpha)$ be the local rectangular Cartesian coordinate system for a pair of microcracks Ω_α with x_1^α axis being identical with the x_1 axis of the global coordinate system, see Fig. 1. The unit base vectors are $\overrightarrow{e_i^\alpha}$ $(i = 1, 2, 3)$ and the origin O_α is at the centre of the inclusion. The

pair of microcracks Ω_α lies in the x_1^α, x_2^α-plane and the unit normal $\overrightarrow{n}\left(\equiv \overrightarrow{e_3^\alpha}\right)$ is in the x_3^α direction. The contribution to the additional average strain rate by a pair of microcrack Ω_α , $\dot{\overline{\varepsilon}}^\alpha$, is defined by

$$\dot{\overline{\varepsilon}}_{ij}^{\alpha} = \frac{1}{\left(\frac{l}{2}\right)^3} \int\limits_{\partial\Omega_\alpha^+} \left(n_i \left[\dot{u}_j\right] + \left[\dot{u}_i\right] n_j\right) dS = H_{ijkl}^{\alpha}\, \dot{\overline{\sigma}}_{kl}, \tag{10}$$

where the components of the constant tensor, H_{ijkl}^{α}, are expressed in the local $\alpha-$coordinates. The additional average strain rate of matrix $\dot{\overline{\varepsilon}}^{MC}$ can be expressed as

$$\dot{\overline{\varepsilon}}^{MC} = \frac{f}{2\pi} \int\limits_0^{2\pi} \dot{\overline{\varepsilon}}_{ij}^{\alpha}\, \overrightarrow{e_i^\alpha}\left(\theta\right) \otimes \overrightarrow{e_j^\alpha}\left(\theta\right) d\theta, \tag{11}$$

where f is the crack density parameter $f = N\left(\frac{l}{2}\right)^3$ with N denoting the total number of pairs of microcracks per unit volume and $\overrightarrow{e_i^\alpha}\left(\theta\right)$ and are the local base vectors. N relates to the inclusion's concentration c and inclusion's radius R by

$$N = \frac{3c}{4\pi R^3}.$$

The solution to the microfractured matrix-inclusions system is the superposition of two problems: i) matrix with the additional strain rate $\dot{\overline{\varepsilon}}^{MC}$, ii) matrix + inclusions with the rate of eigenstrain $\dot{\varepsilon}^*$ which is introduced in order to homogenize the solid, and the rate of stress-free inelastic transformation strain $\dot{\varepsilon}^p - \dot{\overline{\varepsilon}}^\alpha$, where $\dot{\varepsilon}^p$ results from the plastic deformation of inclusions. Let us follow the solution to the problem ii). Eshelby's equivalence principle (3) becomes:

$$\begin{aligned} \dot{\sigma}^{(in)} &= \dot{\overline{\sigma}} + \dot{\tilde{\sigma}} + \dot{\sigma}^{(pt)} = L^1 : \left(\dot{\varepsilon}^0 + \dot{\tilde{\varepsilon}} + \dot{\varepsilon}^{(pt)} - \left(\dot{\varepsilon}^p - \dot{\overline{\varepsilon}}^\alpha\right)\right) = \\ &= L^0 : \left(\dot{\varepsilon}^0 + \dot{\tilde{\varepsilon}} + \dot{\varepsilon}^{(pt)} - \dot{\varepsilon}^* - \left(\dot{\varepsilon}^p - \dot{\overline{\varepsilon}}^\alpha\right)\right). \end{aligned} \tag{12}$$

Eshelby's solution provides the relation

$$\dot{\varepsilon}^{(pt)} = S : \left(\dot{\varepsilon}^* + \dot{\varepsilon}^p - \dot{\overline{\varepsilon}}^\alpha\right) \tag{13}$$

and, in a similar manner to Eq. (7) we arrive at

$$\dot{\tilde{\varepsilon}} = -c\left(S - I\right) : \left(\dot{\varepsilon}^* + \dot{\varepsilon}^p - \dot{\overline{\varepsilon}}^\alpha\right). \tag{14}$$

Substituting (13) and (14) into (12) one gets the equation

$$\begin{aligned} L^1 \,:\, &\left[\dot{\varepsilon}^0 + \left(1-c\right) S : \left(\dot{\varepsilon}^* + \dot{\varepsilon}^p - \dot{\overline{\varepsilon}}^\alpha\right) + c\left(\dot{\varepsilon}^* + \dot{\varepsilon}^p - \dot{\overline{\varepsilon}}^\alpha\right) - \left(\dot{\varepsilon}^p - \dot{\overline{\varepsilon}}^\alpha\right)\right] = \\ = \; & L^0 : \left(\dot{\varepsilon}^0 + \left(1-c\right)\left(S - I\right) : \left(\dot{\varepsilon}^* + \dot{\varepsilon}^p - \dot{\overline{\varepsilon}}^\alpha\right)\right), \end{aligned} \tag{15}$$

which can again be solved for $\dot{\varepsilon}^*$. For further analysis it is convenient to decompose isotropic 4-th-rank tensors L^1 , L^0 and S into hydrostatic and deviatoric parts as

$$L^1 = \left(3\kappa_1, 2\mu_1\right), L^0 = \left(3\kappa_0, 2\mu_0\right), S = \left(\alpha_0, \beta_0\right), \tag{16}$$

with $\alpha_0 = \frac{1}{3}\frac{1+\nu_0}{1-\nu_0}$, $\beta_0 = \frac{2}{15}\frac{4-5\nu_0}{1-\nu_0}$.
The hydrostatic part of stress rate inside the inclusion then becomes

$$\dot{\sigma}_{kk}^{(in)} = \dot{\overline{\sigma}}_{kk}\left[1 - \frac{(1-c)(1-\alpha_0)}{(1-c)(1-\alpha_0)+\frac{\kappa_1}{\kappa_0-\kappa_1}}\right] + \frac{\frac{3\kappa_0\kappa_1}{\kappa_0-\kappa_1}(1-c)(1-\alpha_0)\,\dot{\overline{\varepsilon}}_{kk}^{\alpha}}{(1-c)(1-\alpha_0)+\frac{\kappa_1}{\kappa_0-\kappa_1}} \tag{17}$$

and the deviatoric part of the stress rate

$$\dot{\sigma}_{ij}^{\prime(in)} = \dot{\overline{\sigma}}_{ij}^{\prime}\left[1 - \frac{(1-c)(1-\beta_0)}{(1-c)(1-\beta_0)+\frac{\mu_1}{\mu_0-\mu_1}}\right] - \frac{\frac{2\mu_1\mu_0}{\mu_0-\mu_1}(1-c)(1-\beta_0)\left(\dot{e}_{ij}^{p} - \dot{\overline{e}}_{ij}^{\alpha}\right)}{(1-c)(1-\beta_0)+\frac{\mu_1}{\mu_0-\mu_1}}. \tag{18}$$

It is assumed that the relevant physical law of plastic flow in the inclusions is the J_2-flow theory defined by

$$f = \frac{3}{2}\sigma_{ij}^{\prime(in)}\sigma_{ij}^{\prime(in)} - k^2(\gamma), \tag{19}$$

where $\sigma_{ij}^{\prime(in)}$ follows from Eq. (18), $k(\gamma)$ stands for the radius of the yield surface and represents the isotropic hardening of inclusions with $\gamma = \sqrt{\frac{2}{3}e_{ij}^{p}e_{ij}^{p}}$ being the effective plastic strain. (Note that the residual stresses due to the adjacent brittle matrix are automatically introduced via the composite model.) It may prove advantageous to specialize the evolution of $k(\gamma)$ by means of an equation similar to that employed for kinematic hardening as suggested by Lemaitre and Chaboche [3] $\frac{dk}{d\gamma} = b(Q-k)$, where b and Q are two constants. Q is the asymptotic value which corresponds to a regime of stabilized cycles, and b indicates the speed of the stabilization. This evolution law is quite a good representation of the cyclic hardening effects. Assuming the normality rule, the plastic strain rate is defined as

$$\dot{e}_{ij}^{p} = \lambda\frac{\partial f}{\partial\sigma_{ij}^{\prime(in)}} = \left\{\begin{array}{ll} \frac{3}{2}\frac{\sigma_{ij}^{\prime(in)}\sigma_{kl}^{\prime(in)}\dot{\sigma}_{kl}^{\prime(in)}}{k^2h}, & \text{for } f=0 \text{ and } \sigma_{kl}^{\prime(in)}\dot{\sigma}_{kl}^{\prime(in)} \geq 0 \\ 0, & \text{for } f<0 \text{ or } \sigma_{kl}^{\prime(in)}\dot{\sigma}_{kl}^{\prime(in)} < 0 \end{array}\right\} \tag{20}$$

where $h = \frac{dk}{d\gamma}$.

The overall strain rate $\dot{\overline{\varepsilon}}$ is given by the weighted average of its constituents coupled with averaging over the orientations of local coordinate system and by the superposition of the problems i) and ii); in the global coordinate system this leads to

$$\begin{aligned} \dot{\overline{\varepsilon}}_{kk} &= \dot{\varepsilon}_{kk}^{0} + \dot{\overline{\varepsilon}}_{kk}^{MC} + c\frac{\dot{\varepsilon}_{kk}^{0} - \frac{\kappa_1}{\kappa_0-\kappa_1}\dot{\overline{\varepsilon}}_{kk}^{\alpha}}{(1-c)(1-\alpha_0)+\frac{\kappa_1}{\kappa_0-\kappa_1}}, \\ \dot{\overline{e}}_{ij} &= \dot{e}_{ij}^{0} + \dot{\overline{e}}_{ij}^{MC} + c\frac{\dot{e}_{ij}^{0}}{(1-c)(1-\beta_0)+\frac{\mu_1}{\mu_0-\mu_1}} + c\frac{\frac{\mu_1}{\mu_0-\mu_1}\left(\dot{e}_{ij}^{p} - \dot{\overline{e}}_{ij}^{\alpha}\right)\frac{1}{2\pi}\int_0^{2\pi}\overrightarrow{e_i^{\alpha}}(\theta)\otimes\overrightarrow{e_j^{\alpha}}(\theta)\,d\theta}{(1-c)(1-\beta_0)+\frac{\mu_1}{\mu_0-\mu_1}}. \end{aligned} \tag{21}$$

If microcracks were absent (i.e. $\dot{\overline{\varepsilon}}^{\alpha} \equiv 0$), then one could readily integrate Eqs. (18), (20) and (21). Consider the case of uniaxial loading $\overline{\sigma}_{11} \neq 0$, $\overline{\sigma}_{ij} = 0$ for $i \neq 1, j \neq 1$. Hence, the nonzero deviatoric parts of $\overline{\sigma}_{ij}$ follow as $\overline{\sigma}_{11}^{\prime} = \frac{2}{3}\overline{\sigma}_{11}, \overline{\sigma}_{22}^{\prime} = \overline{\sigma}_{33}^{\prime} = -\frac{1}{3}\overline{\sigma}_{11}$. The average strain rate component $\dot{\overline{\varepsilon}}_{11}$ follows from (21) as

$$\begin{aligned} \dot{\overline{\varepsilon}}_{11} &= \frac{\dot{\overline{\sigma}}_{11}}{9\kappa_0}\left[1 + \frac{c}{(1-c)(1-\alpha_0)+\frac{\kappa_1}{\kappa_0-\kappa_1}}\right] + \frac{\dot{\overline{\sigma}}_{11}}{3\mu_0}\left[1 + \frac{c}{(1-c)(1-\beta_0)+\frac{\mu_1}{\mu_0-\mu_1}}\right] + \\ &\quad + \frac{c\mu_1\,\dot{e}_{11}^{p}}{(1-c)(1-\beta_0)(\mu_0-\mu_1)+\mu_1}. \end{aligned} \tag{22}$$

Eqs. (22), (20) and (18) were numerically integrated using the Runge-Kutta method of 5th order. The elastic constants of constituents were taken as follows: $\mu_0 = 300\ GPa$, $\mu_1 = 84\ GPa$, $\kappa_0 = 400\ GPa$, $\kappa_1 = 200\ GPa$ which correspond to cermet WC-Co. The volume fraction of Co inclusions $c = 0.2$. The ratio of the compression amplitude $|\overline{\sigma}_{11m}|$ to the initial radius of the yield surface $k(0)$ fulfilled the necessary condition for the occurrence of the ratchetting effect

$$\frac{|\overline{\sigma}_{11m}|}{k(0)} > \frac{2}{1 - \frac{(1-c)(1-\beta_0)}{(1-c)(1-\beta_0)+\frac{\mu_1}{\mu_0-\mu_1}}}, \tag{23}$$

i.e. the stress range is more than double of the initial radius of the overall yield surface of composite solid. The constants from the cyclic hardening rule Q and b ranged as follows: $\frac{Q}{k(0)} - 1 \in \langle 0.08, 0.20\rangle$, $b \in \langle 10, 60\rangle$; however, no significant influence upon the overall stress-strain curves was observed. The predicted overall stress-strain curves have not shown any ratchetting. An accumulation of the overall plastic strain due to nonzero mean stress occurs only in the very first cycle, in the next cycles a perfect plastic or elastic shakedown follows and cyclic deformation is purely elastic. It should be noted that almost the same response results when, in addition, the kinematic hardening in the inclusion is considered. The yield function of the J_2-flow theory is then defined by

$$f = \frac{3}{2}\left(\sigma_{ij}^{\prime(in)} - R_{ij}\right)\left(\sigma_{ij}^{\prime(in)} - R_{ij}\right) - k^2(\gamma), \tag{24}$$

where R_{ij} indicates the translation of the yield surface and physically represents the back stress acting on pinned or piled-up dislocations and evolves according to the Armstrong and Frederick's [1] translation rule

$$\dot{R}_{ij} = K\ \dot{e}_{ij}^{p}\ - K_e R_{ij}\dot{\gamma}, \tag{25}$$

where the second term (called the dynamic recovery) describes the evanescence of the strain memory as well as the strain hardening, K and K_e are material parameters, see [2] or [3]. It is well-known that the AF model overpredicts ratchetting in most situation because the dynamic recovery term is too active. In our computations the material parameters K and K_e were changed in a wide range, however no ratchetting was predicted. This is due to a strong plastic constraint exerted by matrix on inclusions.

It will be shown in the next that microcracks emanating from the poles of a inclusion, see Fig. 1, can promote ratchetting of composite. However, the system of preceding equations is not sufficient to calculate this response. To complete the formulation, we must relate the strain rate $\dot{\overline{\varepsilon}}^{\alpha}$ to the eigenstrain rate $\dot{\varepsilon}^{*}$, to the plastic strain rate $\dot{e}^{p}$ and to the applied stress rate $\dot{\overline{\sigma}}$. We shall do this by calculating the approximative opening stress intensity factor, K_I, at the tips of the pair of flat microcracks emanating from the poles of a spherical inclusion in two different ways: (1) by expressing the local stress field of the inclusion and the Green's function for a microcrack embedded in this stress field, and (2) by calculating the stress intensity factor associated with the gap of the microcrack faces at the matrix/inclusion interface (so called dislocated crack) Δ_{PC}, see Fig. 1.

Ad 1. For simplicity we assume only simple compression acting in the direction of x_1 axis of the global coordinate system which, as it was already specified, coincides with x_1^{α} axis of a local coordinate system. The stresses are concentrated by the inclusion under

simple compression such that, the hoop stresses along the interface at inclusion's north and south poles are tensile. For an unbounded solid one can calculate the stresses outside the inclusion using the Eshelby tensor field $S^{\infty}_{ijkl}\left(\overrightarrow{r};\Omega\right)$ [8], where $\overrightarrow{r}$ denotes the radius vector of the point in the matrix and Ω denotes the inclusion. The stress intensity factor K_I for a pairof flat cracks emanating from the poles of a spherical inclusion can be found by using a similar approximative method already applied to a spherical hole by Sammis and Ashby [9]. Approximative stress intensities can be found from the Green's function for a crack embedded in the stress field of the inclusion. In doing this the integral over the face of the microcrack is approximated by an integral along the line of the maximum tensile stress,

$$K_I = \sqrt{\frac{R}{\pi L}} \int\limits_{-L}^{L} L^0_{33ij} S^{\infty}_{ijkl}\left(\overrightarrow{r};\Omega\right)\left(\varepsilon^*_{kl} + \varepsilon^p_{kl} - \delta_{k3}\delta_{l3}\overline{\varepsilon}^{\alpha}_{33}\right)\left(\frac{L+X}{L-X}\right)^{1/2} dX, \tag{26}$$

because the stresses are so sharply peaked near the poles of the inclusion that other geometric considerations are of minor importance. L in Eq. (26) denotes the normalized crack length $L = \frac{l}{R}$.

Ad 2. The Mode I stress intensity factor associated with the gap of the microcrack faces at the matrix/inclusion interface (there is no contribution from the applied stresses under simple compression acting in the direction of x^{α}_1) is estimated by [10]

$$K'_I\left(\Delta_{PC}\right) = \frac{1}{2}\frac{\mu_0}{1-\nu_0}\frac{\Delta_{PC}}{\sqrt{\pi l}}. \tag{27}$$

Δ_{PC} can be related to the additional strain of the inclusion $\Delta\varepsilon^{PC}_{33}$ generated by microcracks

$$\Delta\varepsilon^{PC}_{33} = \varepsilon^{PC}_{33}\left(\overline{\varepsilon}^{\alpha}_{33} \neq 0\right) - \varepsilon^{PC}_{33}\left(\overline{\varepsilon}^{\alpha}_{33} = 0\right), \tag{28}$$

where

$$\varepsilon^{PC}_{33} = \varepsilon^0_{33} + \widetilde{\varepsilon}_{33} + \varepsilon^{(pt)}_{33} + \overline{\varepsilon}^{\alpha}_{33} \tag{29}$$

is the component of the total strain of the inclusion in the x^{α}_3 direction. For $\Delta\varepsilon^{PC}_{33}$ it follows

$$\begin{aligned}\Delta\varepsilon^{PC}_{33} \;=\; & \overline{\varepsilon}^{\alpha}_{33} - \frac{1}{3}\left[\alpha_0\left(1-c\right)+c\right]\frac{\frac{\kappa_1}{\kappa_0-\kappa_1}\overline{\varepsilon}^{\alpha}_{33}}{\left(1-c\right)\left(1-\alpha_0\right)+\frac{\kappa_1}{\kappa_0-\kappa_1}} + \\ & + \left[\beta_0\left(1-c\right)+c\right]\frac{\frac{\mu_1}{\mu_0-\mu_1}\left[e^p_{33}\left(\overline{\varepsilon}^{\alpha}_{33}\neq 0\right) - e^p_{33}\left(\overline{\varepsilon}^{\alpha}_{33}=0\right) - \frac{2}{3}\overline{\varepsilon}^{\alpha}_{33}\right]}{\left(1-c\right)\left(1-\beta_0\right)+\frac{\mu_1}{\mu_0-\mu_1}},\end{aligned} \tag{30}$$

where to the order of $O\left(\overline{\varepsilon}^{\alpha}_{33}\right)$is

$$e^p_{33}\left(\overline{\varepsilon}^{\alpha}_{33}\neq 0\right) - e^p_{33}\left(\overline{\varepsilon}^{\alpha}_{33}=0\right) - \frac{2}{3}\overline{\varepsilon}^{\alpha}_{33} \approx 0.$$

The additional strain of the inclusion $\Delta\varepsilon^{PC}_{33}$ and the gap of the microcrack faces at the matrix/inclusion interface Δ_{PC} can be related under the assumption that the gap Δ_{PC} is constant across the inclusion by modifying Eq. (10)

$$\Delta\varepsilon^{PC}_{33} = \frac{1}{R^3}\int\limits_S \Delta_{PC} dS = \frac{\pi}{R}\Delta_{PC}, \tag{31}$$

where R stands for the inclusion's radius and S denotes the inclusion's cross-section. Hence

$$\Delta_{PC} = \frac{R}{\pi}\overline{\varepsilon}^{\alpha}_{33}\left\{1 - \frac{\left[\alpha_0\left(1-c\right)+c\right]\frac{\kappa_1}{\kappa_0-\kappa_1}}{3\left[\left(1-c\right)\left(1-\alpha_0\right)+\frac{\kappa_1}{\kappa_0-\kappa_1}\right]}\right\}. \tag{32}$$

To obtain a relation between the strain rate $\dot{\overline{\varepsilon}}^{\alpha}$ on the one side and the eigenstrain rate $\dot{\varepsilon}^{*}$, the plastic strain rate $\dot{e}^{p}$ and the applied stress rate $\dot{\overline{\sigma}}$ on the other side, we require

$$K_I = K_I'. \tag{33}$$

By time differentiation of (33) and substituting for $\dot{\varepsilon}^{*}_{kk}$, $\dot{e}^{*}_{11}+\dot{e}^{p}_{11}$ and $\dot{e}^{*}_{33}+\dot{e}^{p}_{33}$ a required relation for $\dot{\overline{\varepsilon}}^{\alpha}_{33}$ is obtained:

$$\dot{\overline{\varepsilon}}^{\alpha}_{33} = \frac{1}{d_4}\left(d_1\,\dot{e}^{p}_{11} + d_2\,\dot{e}^{p}_{33} + d_3\,\dot{\overline{\sigma}}_{11}\right), \tag{34}$$

where

$$\begin{aligned} d_1 &= d_1\left(\kappa_0,\mu_0,c,L\right),\ d_2 = d_2\left(\kappa_0,\mu_0,c,L\right), \\ d_3 &= d_3\left(\kappa_0,\mu_0,c,L\right),\ d_4 = d_4\left(\kappa_0,\mu_0,c,L\right) \end{aligned}$$

are complicated functions of the elastic constants of the matrix, of the volume fraction of inclusions c and of the relative microcrack length L.

NUMERICAL RESULTS AND DISCUSSION

As already noted, in the case of uniaxial loading $\overline{\sigma}_{11} \neq 0$ the only nonzero component of $\overline{\varepsilon}^{\alpha}_{kl}$ is $\overline{\varepsilon}^{\alpha}_{33}$. One can then easily prove using Eq. (11) that $\dot{\overline{\varepsilon}}^{MC}_{11} = 0$. The overall strain rate component $\dot{\overline{\varepsilon}}_{11}$ follows from (21) as

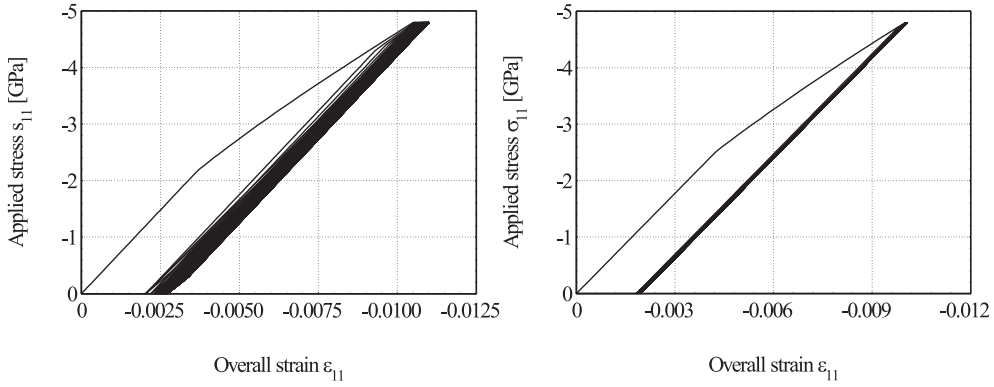

a) b)

Fig. 2. Predicted overall stress-strain curves for the first $N = 100$ cycles, microcracking present in the matrix: a) $b = 10$, $Q/k\left(0\right) - 1 = 0.08$, $\left|\overline{\sigma}_{11m}\right|/k\left(0\right) = 3.7$, $L = 3$, b) $b = 10$, $Q/k\left(0\right) - 1 = 0.13$, $\left|\overline{\sigma}_{11m}\right|/k\left(0\right) = 3.2$, $L = 3$.

$$\dot{\overline{\varepsilon}}_{11} = \frac{\dot{\overline{\sigma}}_{11}}{9\kappa_0}\left[1+\frac{c}{\left(1-c\right)\left(1-\alpha_0\right)+\frac{\kappa_1}{\kappa_0-\kappa_1}}\right] + \frac{1}{3}\frac{c\frac{\kappa_1}{\kappa_0-\kappa_1}\,\dot{\overline{\varepsilon}}^{\alpha}_{33}}{\left(1-c\right)\left(1-\alpha_0\right)+\frac{\kappa_1}{\kappa_0-\kappa_1}} + \\ + \frac{\dot{\overline{\sigma}}_{11}}{3\mu_0}\left[1+\frac{c}{\left(1-c\right)\left(1-\beta_0\right)+\frac{\mu_1}{\mu_0-\mu_1}}\right] + \frac{c\mu_1\left(\dot{e}^{p}_{11}-\dot{\overline{e}}^{\alpha}_{11}\right)}{\left(1-c\right)\left(1-\beta_0\right)\left(\mu_0-\mu_1\right)+\mu_1}. \tag{35}$$

Eqs. (35), (34), (20) and (18) were numerically integrated using the Runge-Kutta method of 5th order to obtain the uniaxial stress-strain curves under cyclic loading. The elastic constants of constituents were taken as formerly: $\mu_0 = 300\ GPa$, $\mu_1 = 84\ GPa$, $\kappa_0 = 400\ GPa$, $\kappa_1 = 200\ GPa$. Also the same values of the volume fraction of inclusions, the ratio of the compression amplitude to the initial radius of the yield surface and the constants from the cyclic hardening rule were used as in the previous computations related to the case without microcracking. The normalized crack length $L = \frac{l}{R}$ was considered from the interval $\langle 1, 3\rangle$. Two of the predicted overall stress-strain curves are shown in Fig. 2. Contrary to the results of the computations related to no microcracking a strong influence of the parameters $\frac{|\overline{\sigma}_{11m}|}{k(0)}$, $\frac{Q}{k(0)} - 1$, b and L on the overall stress-strain curves was observed.

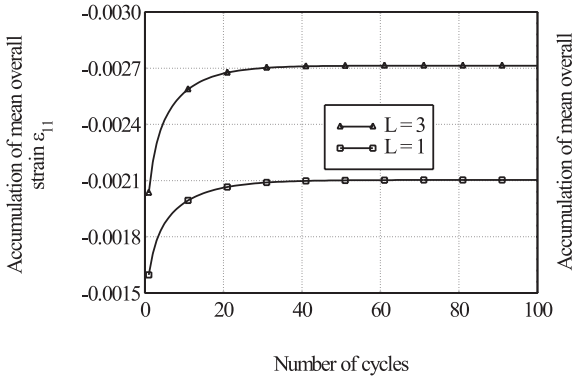

Fig. 3. Accumulation of the permanent mean overall strain $\overline{\varepsilon}_{11}$. b=10, $Q/k\,(0)$-1=0.08, $|\overline{\sigma}_{11m}|\,/k\,(0)$ =3.7.

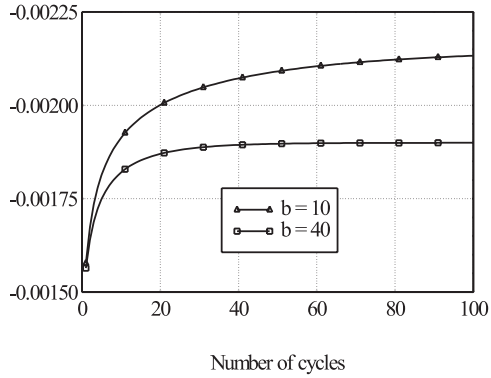

Fig. 4. Accumulation of the permanent mean overall strain $\overline{\varepsilon}_{11}$. $Q/k\,(0)$-1=0.08, $|\overline{\sigma}_{11m}|\,/k\,(0)$ =3.6, L=1.

Figs. 3-5 illustrate an effect of these parameters upon the accumulation of a mean overall strain in each cycle. It is seen that these parameters significantly affect both the length of the period of a pronounced ratchetting and the value of the accumulated overall strain. Note a peculiar influence of the parameter $\frac{Q}{k(0)} - 1$ upon the value of the accumulated mean overall strain. Fig. 5 shows that an increase of $\frac{Q}{k(0)} - 1$ (i.e. a relative increase of the asymptotic value of $k\,(\gamma)$ with respect to the initial one) may sometimes result in an increasing and sometimes in a decreasing value of the accumulated overall strain depending on the values of other parameters.

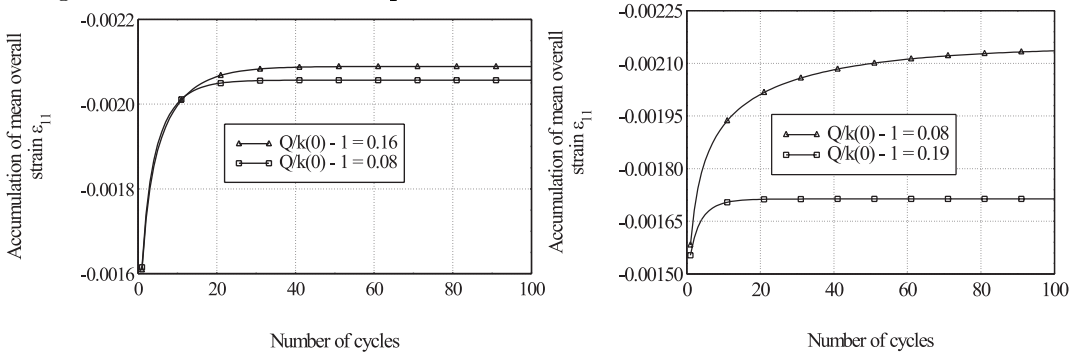

Fig. 5. Accumulation of the permanent mean overall strain $\overline{\varepsilon}_{11}$. a) $b = 10$, $|\overline{\sigma}_{11m}|\,/k\,(0) = 3.84$, $L = 1$, b) $b = 40$, $|\overline{\sigma}_{11m}|\,/k\,(0) = 3.7$, $L = 1$.

The explanation of this phenomenon is postponed to the final part of this section. Figs. 3-5 indicate that the ratchetting is followed by an almost perfect plastic or elastic shake-down which will be also discussed later on.

This is matter of interest to make clear why the developed model can describe ratchetting effects even though the plastic flow within inclusions is described by the isotropic hardening rule (20). To this end, substitute (18) into (20), make use of Eq. (34) and, within the uniaxial loading context, obtain after solving for $\dot{e}^p_{11}$, $\dot{e}^p_{22}$ and $\dot{e}^p_{33}$:

$$\begin{aligned}
\dot{e}^p_{11} &= \frac{3}{2}\frac{\sigma'^{(in)}_{11}\,\dot{\overline{\sigma}}_{11}\left(A\sigma'^{(in)}_{11}+B\frac{d_3}{d_4}\sigma'^{(in)}_{33}\right)}{k^2 h_{ef}},\\
\dot{e}^p_{22} &= \frac{3}{2}\frac{\sigma'^{(in)}_{22}\,\dot{\overline{\sigma}}_{11}\left(A\sigma'^{(in)}_{11}+B\frac{d_3}{d_4}\sigma'^{(in)}_{33}\right)}{k^2 h_{ef}},\\
\dot{e}^p_{33} &= \frac{3}{2}\frac{\sigma'^{(in)}_{33}\,\dot{\overline{\sigma}}_{11}\left(A\sigma'^{(in)}_{11}+B\frac{d_3}{d_4}\sigma'^{(in)}_{33}\right)}{k^2 h_{ef}},
\end{aligned} \tag{36}$$

where

$$A = 1-\frac{(1-c)(1-\beta_0)}{(1-c)(1-\beta_0)+\frac{\mu_1}{\mu_0-\mu_1}},\ B=\frac{\frac{2\mu_1\mu_0}{\mu_0-\mu_1}(1-c)(1-\beta_0)}{(1-c)(1-\beta_0)+\frac{\mu_1}{\mu_0-\mu_1}}$$

and

$$h_{ef}=\frac{dk}{d\gamma}+B-\frac{3}{2}\frac{B}{k^2}\left(\frac{d_1}{d_4}\sigma'^{(in)}_{11}\sigma'^{(in)}_{33}+\frac{d_2}{d_4}\left(\sigma'^{(in)}_{33}\right)^2\right) \tag{37}$$

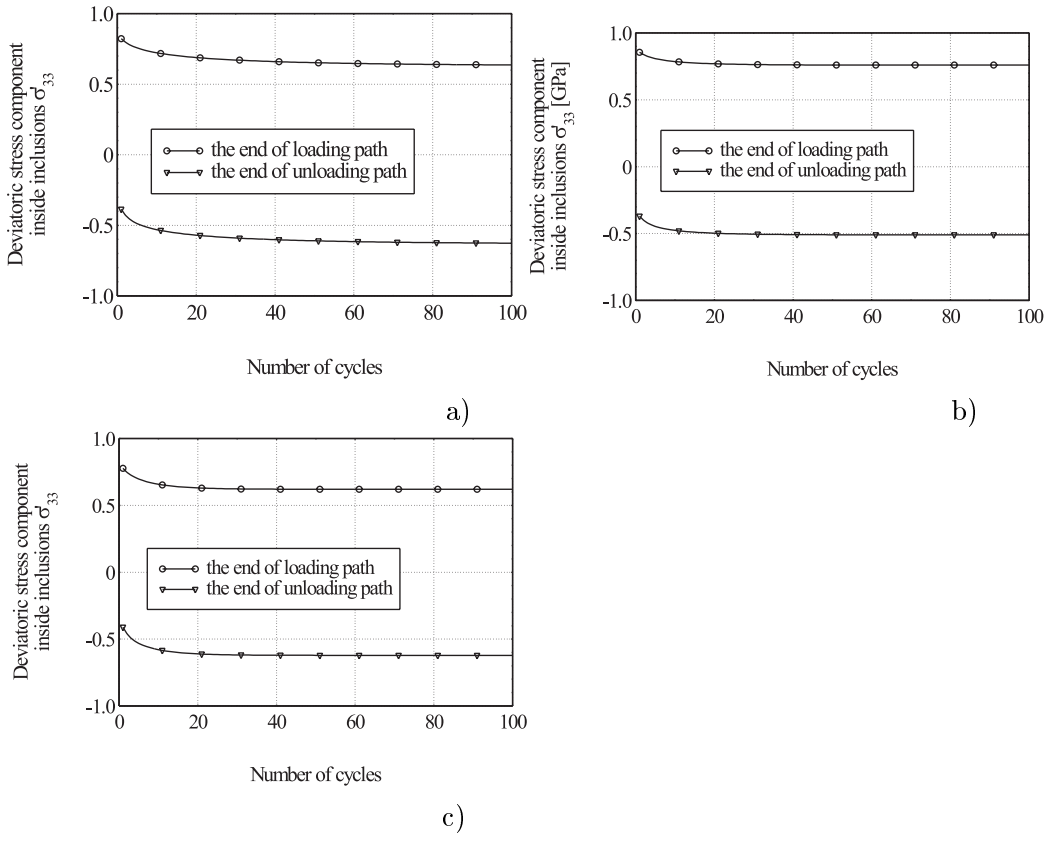

Fig. 6. Evolution of the deviatoric stress component inside inclusions $\sigma'^{(in)}_{33}$. a) $b=40$, $Q/k\,(0)-1=0.08$, $|\overline{\sigma}_{11m}|/k\,(0)=3.7$, $L=1$, b) $b=40$, $Q/k\,(0)-1=0.08$, $|\overline{\sigma}_{11m}|/k\,(0)=3.6$, $L=1$, c) $b=10$, $Q/k\,(0)-1=0.08$, $|\overline{\sigma}_{11m}|/k\,(0)=3.84$, $L=1$.

is the effective hardening modulus. Note that $\frac{d_2}{d_4}>0$, $\frac{d_1}{d_4}>0$ while $\frac{d_2}{d_4}\gg\frac{d_1}{d_4}$. The hardening modulus in (37) has a similar mathematical structure as the hardening modulus in the classical model of plastic flow with nonlinear kinematic hardening which evolves according

to the (AF) translation rule (25). Let k_1 is the point in overall stress space where yielding of inclusions initiates prior to approaching the bound $\overline{\sigma}_{11m}$ in compression. Similarly, k_2 is the corresponding point on the unloading path for the onset of yield prior to reaching the zero load. The value of the effective hardening modulus h_{ef} changes between k_1 and $\overline{\sigma}_{11m}$ and between k_2 and 0 according to the changes of the values the deviatoric stress components inside the inclusion $\sigma_{11}^{\prime(in)}$ and $\sigma_{33}^{\prime(in)}$. Since the values of $\sigma_{11}^{\prime(in)}$ and $\sigma_{33}^{\prime(in)}$ are of the same order and since $\frac{d_2}{d_4} \gg \frac{d_1}{d_4}$, it follows that the component $\sigma_{33}^{\prime(in)}$ is dominant one. Therefore, if the absolute value of the deviatoric stress component $\left|\sigma_{33}^{\prime(in)}\right|$ on the loading path $\langle k_1, \overline{\sigma}_{11m}\rangle$ is higher than that for the unloading path $\langle k_2, 0\rangle$, then the hardening modulus h_{ef} is smaller

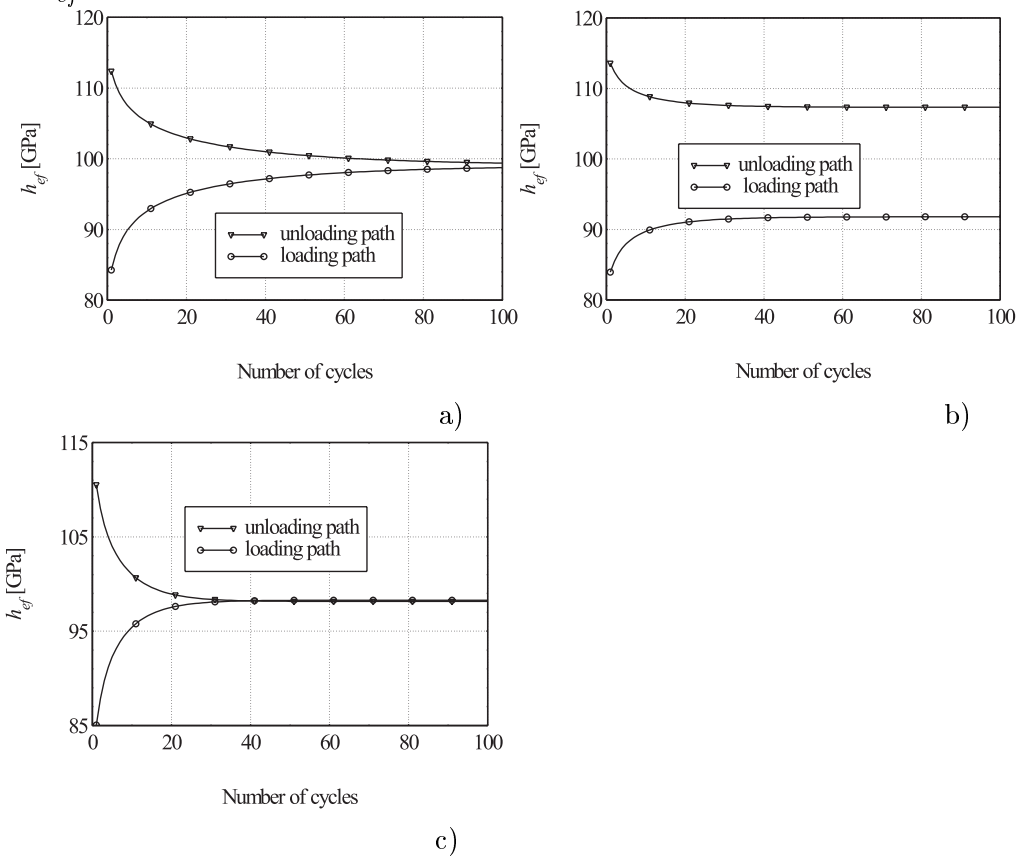

Fig. 7. Evolution of the effective hardening modulus h_{ef} a) $b = 40$, $Q/k\,(0) - 1 = 0.08$, $|\overline{\sigma}_{11m}|\,/k\,(0) = 3.7$, $L = 1$, b) $b = 40$, $Q/k\,(0) - 1 = 0.08$, $|\overline{\sigma}_{11m}|\,/k\,(0) = 3.6$, $L = 1$, c) $b = 10$, $Q/k\,(0) - 1 = 0.08$, $|\overline{\sigma}_{11m}|\,/k\,(0) = 3.84$, $L = 1$.

for the stress states lying on the loading path than for the unloading path. The cyclic loops, therefore, are not closed and they progressively shift in the direction of the negative overall strain axis. If with the continued shift the value of $\left|\sigma_{33}^{\prime(in)}\right|$ decreases on the loading path $\langle k_1, \overline{\sigma}_{11m}\rangle$ and increases on the unloading path $\langle k_2, 0\rangle$ then the effective hardening modulus on the loading path increases and for the unloading path decreases cycle by cycle. In the end, the hardening moduli become either equal and the loops become stabilized (plastic shakedown), or the elastic shakedown takes place and the cyclic deformation is purely elastic. Fig. 6 shows the evolution of $\sigma_{33}^{\prime(in)}$ at the compression load bound $\overline{\sigma}_{11m}$ and the residual stress component $\sigma_{33}^{\prime(in)}$ at the zero load during cycling for several combinations of the parameters $\frac{|\overline{\sigma}_{11m}|}{k(0)}$, $\frac{Q}{k(0)} - 1$, b and L. Apparently, two distinctive regimes occur: after some transient period the values of $\sigma_{33}^{\prime(in)}$ stabilizes reaching at the compression bound

and at the zero load either the same absolute value or different absolute values. Fig. 7 shows the evolution of the corresponding effective hardening moduli during cycling. It is seen that the effective hardening moduli become either equal and the plastic shakedown results, or they reach different saturated values. The saturated values of the hardening moduli in the latter case are only fictitious ones because the cyclic deformation is here purely elastic and the hardening modulus thus loses its meaning. Hence, the saturation is just an indicator of elastic shakedown.

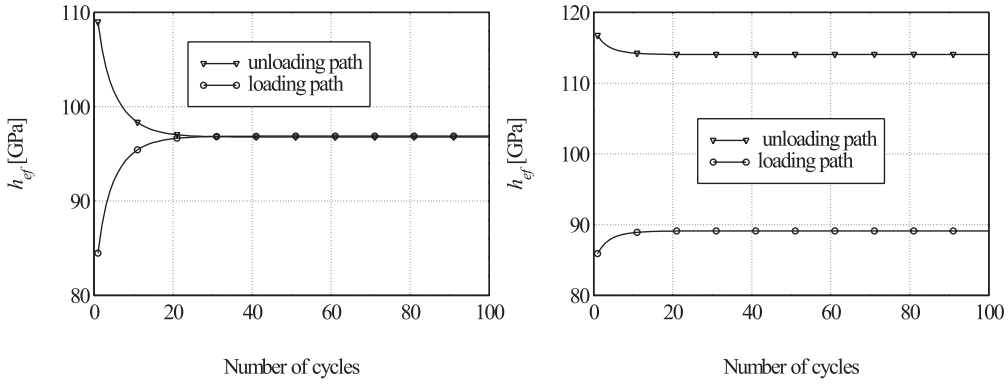

Fig. 8. Evolution of the effective hardening modulus h_{ef} a) $b = 10$, $Q/k\,(0) - 1 = 0.16$, $|\overline{\sigma}_{11m}|\,/k\,(0) = 3.84$, $L = 1$, b) $b = 40$, $Q/k\,(0) - 1 = 0.19$, $|\overline{\sigma}_{11m}|\,/k\,(0) = 3.7$, $L = 1$.

In the light of the preceding discussion we can explain the results displayed in Fig. 5 in the following way: an increase of $\frac{Q}{k(0)} - 1$ generally delays the regime of stabilized cycles, because attaining a higher asymptotic value Q with respect to $k\,(0)$ requires to reach higher plastic strains. As a results, the plastic shakedown either delays, compare Figs. 7c and 8a, or, prior to the plastic shakedown could take place, the elastic shakedown occurs, compare Figs. 7a and 8b. In the former case the accumulation of the mean overall strain is promoted, see Fig. 5a, while in the latter case it stops evolving, see Fig. 5b.

For comparison, a finite element analysis of the investigated problem has been attempted and results are shown in an accompanying paper in the proceedings [11].

Acknowledgments
The support of the Grant Agency of the Czech Republic through grant No. 101/99/0829 is gratefully acknowledged.

REFERENCES

[1] Mori, T., Tanaka, K., Average Stress in Matrix and Average Elastic Energy of Materials with Misffitting Inclusions, *Acta Metallurgica* 21 (1973), 571-574.

[2] Armstrong, P.J., Frederick, C.O., A Mathematical Representation of the Multiaxial Bauschinger Effect. Report RD/B/731, Central Electricity Generating Board, 1966.

[3] Lemaitre, J., Chaboche, J.L., Mechanics of Solid Materials, Cambridge Univ. Press, 1990.

[4] Ohno, N., Current State of the Art in Constitutive Modelling for Ratchetting, Transactions of the 14th Int. Conf. on Structural Mechanics in Reactor Technology (SMiRT 14), Lyon, France, August 17-22, 1997.

[5] Jiang, Y., Sehitoglu, H., Modeling of Cyclic Ratchetting Plasticity, Parts I and II. *J. Appl. Mechanics* 63 (1996), 720-733.

[6] Tandon, G.P. , Weng, G.J., Stress Distribution in and Around Spheroidal Inclusions and Voids at Finite Concentration, *J. Appl. Mechanics* 53 (1986), 511-518.

[7] Nemat-Nasser, S., Hori, M., Micromechanics: Overall Properties of Heterogeneous Materials, North-Holland, 1993.

[8] Eshelby, J.D., The Determination of the Elastic Field of an Ellipsoidal Inclusion, and Related Problems, *Proc. of the Royal Society, Series A* 241 (1957), 376-396.

[9] Sammis, G.S., Ashby, M.F., The Failure of Brittle Porous Solids under Compressive Stress States, *Acta Metallurgica* 34 (1986), 511-526.

[10] Tada, H., Stress Analysis of Cracks Handbook, Del. Research Corp., Hellertown 1973.

[11] Heger, J., Kotoul, M., FE Modelling of Particulate Composites with Brittle Matrix under Cyclic Compression Loading, Proc. of MSFM-3, Brno, Czech Republic, 2001.